Hindawi
Geofluids
Volume 2022, Article ID 2755102, 11 pages
https://doi.org/10.1155/2022/2755102

Research Article

Study on Modified Dynamic Constitutive Model for Calcareous Sand considering Particle Breakage

Huibin Chen,[1] **Heying Hou**,[1] **Pengming Jiang**,[2] **Zhenzhen Nong**,[1] **Tianxiang Li**,[1] **Qing Wang**,[1] **and Zhuojie Pan**[3]

[1]*Jiangsu University of Science and Technology, School of Civil Engineering and Architecture, Zhenjiang 212000, China*
[2]*Suzhou University of Science and Technology, Suzhou 215000, China*
[3]*Nanjing Hydraulic Research Institute, Institute of Geotechnical Engineering, Nanjing 210000, China*

Correspondence should be addressed to Heying Hou; just_hyhou@163.com

Received 7 February 2022; Revised 25 March 2022; Accepted 8 April 2022; Published 26 April 2022

Academic Editor: Xiangguo Kong

Calcareous sand is special sand widely distributed in the South China Sea, which is characterized by the irregular particle shape, high porosity, easy-breaking, etc. Through a series of dynamic triaxial tests, this paper will study the influence of particle breakage on the dynamic deformation characteristics of calcareous sand and explore a modified dynamic constitutive model considering particle breakage suitable for calcareous sand. The research shows that the dynamic deformation characteristics of calcareous sand can be described by the Hardin-Drnevich model. The maximum dynamic shear modulus and average effective stress of calcareous sand obey Janbu empirical formula, with approximate a linear relationship. Through screening experiment, it is found that there is a linear relationship between particle crushing rate and effective confining pressure. On the basis of Hardin-Drnevich, the dynamic constitutive model of calcareous sand considering the influence of particle breakage is established by introducing relative crushing rate Br and constitutive model parameters. By comparing with the experimental data, it is found that the relative error between the calculated value and the experimental value of the model is no more than 12%, and the average error is no more than 8%, indicating that the modified dynamic constitutive model can better predict the dynamic characteristics of calcareous sand.

1. Introduction

The development and construction of islands and reefs in the South China Sea have important and far-reaching strategic significance for China's marine economic development and the maintenance of marine sovereignty. In recent years, reef filling and land reclamation projects in the South China Sea have increased rapidly, and related projects such as airport and wharf have been built [1–3]. Due to the special geographical location and geological structure, the selection of foundation structure on calcareous sand is subject to many restrictions.

Calcareous sand has the main characteristics of large specific gravity, high internal friction angle, irregular shape, and high porosity and is easy to crush and cement [4–6], resulting in significant differences in geotechnical characteristics and basic physical properties of the calcareous sand and general continental sand [7–9]. Compared with quartz sand, calcareous sand has rich pores, sharp edges and corners, and large porosity. Under certain stress, the particles are easy to break, and the plastic deformation is large during compression. Due to the irregular shape of calcareous sand particles, the particle movement under external force is slower than that of quartz sand, which leads to longer compression and consolidation time than that of quartz sand. Also, calcareous sand shows higher compressibility.

The dynamic constitutive model of sand is generally divided into three parts: the viscoelastic model, elastic-plastic model, and nonlinear model. The elastic-plastic model includes a multifacet model, edge interface model, secondary loading surface model, multi mechanism theory, generalized plasticity theory, and intrinsic time theory. Nonlinear models include Martin et al. [10], Li and Wang [11], Zhao et al. [12], and other "true nonlinear" models.

Viscoelastic model is the simplest dynamic constitutive model, and the most commonly used is the Hardin-Drnevich equivalent viscoelastic linear model [13]. This model regards soil as a viscoelastic medium so it can not reflect the permanent deformation of soil. If the influence of soil deformation needs to be considered, other methods can be applied. The Hardin-Drnevich model usually uses dynamic shear modulus G and damping ratio λ to reflect the characteristics of dynamic stress-strain relationship of soil (hysteresis and nonlinearity of soil) and creates the relationship between dynamic shear modulus and dynamic strain function and the relationship between damping ratio and dynamic strain function, respectively. At the same time, the influence of average principal stress is considered in the above relationships. A lot of work has been devoted to development of the dynamic constitutive model. Ishihara et al. [14] applied the revised massing hysteretic rule to the Hardin-Drnevich model to better describe the dynamic stress-strain relationship of soil under dynamic load. Chen et al. [15] improved the damping ratio formula in the Hardin-Drnevich model by adding three parameters related to soil properties. The improved Hardin-Drnevich formula applies to cohesive soil and cohesionless soil. However, there are few studies on the dynamic constitutive model of calcareous sand considering particle breakage under cyclic dynamic load. Through triaxial compression tests on coral sand with different compactness, Liu et al. [16] proposed the critical state line considering particle breakage and the rule of unified hardening parameters and then established an elastic-plastic constitutive model of coral sand considering particle breakage. Chen and Ueng [17] explored the effect of particle breakage on the strength of sand in the process of drained shear through triaxial compression tests of Fulung sand, Tamsui River sand, decomposed granite, and based on Rowe's principle of minimum energy ratio. Hardin proposed a crushing model that could describe the variation of particle crushing under an equal shear stress ratio [18, 19]. For studies on calcareous sand, Wang and Sun [20] considered the coupling effect of particle breakage and slip of calcareous sand samples and established the constitutive relationship of calcareous sand by using the elastic damage model and boundary interface model. Cai et al. [21] discussed the influence of particle breakage on soil deformation and e-p curve through the triaxial test of calcareous sand and established a constitutive model of calcareous sand considering particle breakage. Based on a systematic experimental study on the mechanical properties and particle breakage of calcareous sand under triaxial conditions, Hu [22] established a constitutive model that could consider the particle breakage effect. Comparing with the prediction from finite element analysis, the prediction of stress-strain and volume deformation characteristics of calcareous sand samples under high confining pressure achieved satisfactory results. Wang et al. [23] carried out electron microscope scanning, image analysis, and triaxial drainage test on calcareous sand to explore the influence of particle breakage on the deformation and energy dissipation of calcareous sand. Peng et al. [24] filmed the calcareous sand with different particle sizes before and after the side limit compression test, adopted the ImageJ software for image processing and statistical analysis, and proposed the cumulative crushing rate index of samples considering crushing overlap and masking. To sum up, there are few reports on the dynamic load test of calcareous sand with mixed particle size under complex stress state and attempts to build a viscoelastic dynamic constitutive model of calcareous sand considering particle breakage.

For the dynamic shear modulus and damping ratio of various sands, a large number of experimental research and theoretical derivation have been conducted. Seed et al. [25] provided the test curves of dynamic shear modulus ratio and damping ratio of different sandy soils with strain through compactness and effective stress. Hardin and Black [26] obtained the maximum dynamic shear modulus relationship between void ratio and effective average principal stress of cohesive soil through the experimental study of dynamic modulus and damping ratio of cohesive soil. Zhu and Wu [27] studied the influence of different mechanical factors on the dynamic characteristics of sand and modified the relationship formula of the maximum dynamic shear modulus of sand. Shen [28] and Dong et al. [29] obtained the empirical formula of dynamic modulus and damping ratio of coarse-grained soil. Also, research through dynamic triaxial tests [30–32] further helps enrich the understanding of mechanical properties of calcareous sand.

At present, most of the dynamic constitutive model of calcareous sand ignores the particle breakage effect under dynamic load. It is advisable to adopt the control variable method in which the effective confining pressure is served as an independent variable, which can facilitate the parameter calculation of the dynamic constitutive model. Based on the results from the consolidated undrained dynamic triaxial test, parameters of the particle breakage constitutive model are introduced and expressed quantitatively by a unified formula. The dynamic constitutive model of calcareous sand with different particle sizes considering particle breakage under a certain stress state is established in this paper. This will theoretically support the development of related engineering activities on calcareous sand in the South China Sea island.

2. Dynamic Triaxial Test Scheme

2.1. Test Materials. The calcareous sand used in this test comes from an island and reef in the South China Sea. The particles are relatively dispersed, white, angular, and irregular in shape and have many internal pores. The maximum particle size is 3 mm, and the minimum particle size is 0.25 mm. Particles with size of 2-2.5 mm have the largest share, accounting for 69.72% of the whole, and the particles with size of 0.25-0.5 mm account for the least 0.26%. The maximum dry density of calcareous sand is 1390 kg/m^3, the minimum dry density is 1160 kg/m^3, and the compactness is 75%. The initial gradation of calcareous sand is shown in Figure 1.

2.2. Test Instruments. This test adopts domestic DSZ-2 dynamic triaxial apparatus (triaxial test system of electromagnetic unidirectional vibration) to determine the dynamic characteristic indexes such as failure strength,

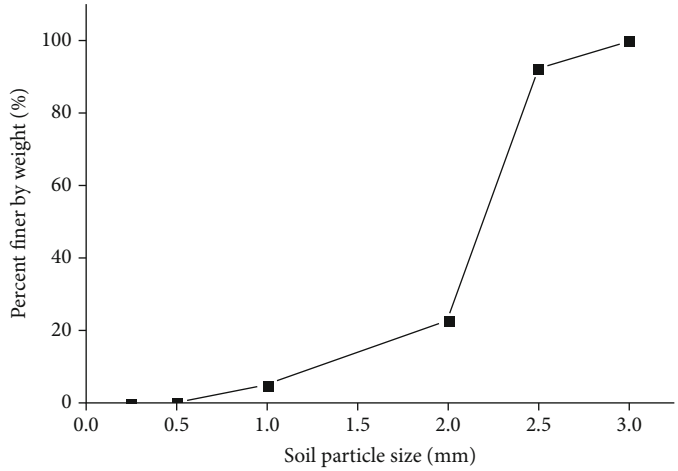

Figure 1: Initial gradation of calcareous sand.

dynamic elastic modulus, and damping ratio of the sample. The DSZ-2 dynamic triaxial apparatus adopts electromagnetic vibration plus dynamic stress and pneumatic plus static force, and the maximum axial dynamic stress is 200 kPa, as shown in Figure 2.

The instrument is mainly composed of six parts: (1) air pump, (2) pressure and drainage system, (3) triaxial chamber, (4) vibration exciter, (5) electrical cabinet, and (6) computer data acquisition and processing.

2.3. Sample Preparation and Saturation. Wash the sample with water and then dry it, screen out five groups of calcareous sand with different particle sizes, weigh its mass, pour it into three ceramic cylinders, stir it evenly with a fine glass rod, pour the above three cylinders of calcareous sand sample into about 2/3 cylinders of distilled water, boil it on the electric furnace for about 30 minutes, and then cool it to normal temperature (remove part of the internal pores of calcareous sand).

The size of the above sample is 50 mm ∗ 100 mm. According to the operation specification of the geotechnical test, first put the latex film on the lower indenter, clamp the bottom end with a rubber band, then clamp the split mold on both sides of the latex film, buckle the upper end of the latex film on the top of the split mold, and suck the exhaust pipe outside the split mold with a vacuum pump to tighten the inner latex film and to make the inner membrane closely fit with the split mold, At this time, the cooled calcareous sand is vibrated into the rubber mold in three equal times. After all the calcareous sand is installed, open the upper drain valve and carefully remove the split mold to avoid disturbance to the sample (as shown in Figure 3). After sample installation, the sample is saturated by the method of water head saturation and then back pressure saturation. When saturation $S_r > 95\%$, the sample is considered to be saturated.

2.4. Sample Scheme. To study the effect of effective consolidation stress on dynamic shear modulus and damping ratio of calcareous sand under cyclic dynamic load, the control

Figure 2: DSZ-2 schematic configuration of the experiment.

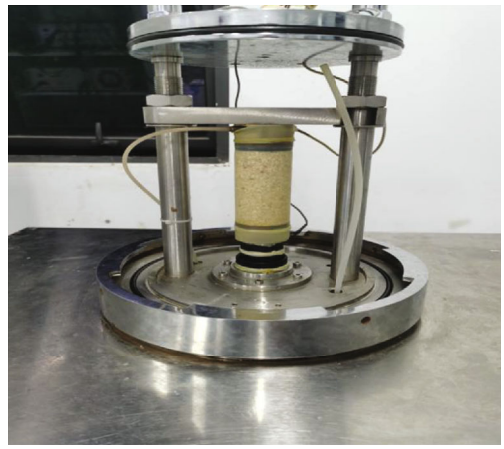

Figure 3: Calcareous sand sample map.

variable method is adopted. Among them, the density of calcareous sand is 1320 kg/m^3, and four effective confining pressures (100 kPa, 200 kPa, 300 kPa, and 400 kPa) are adopted in the test. After the sample is saturated and consolidated under constant pressure for more than 1 h, the volume transformer reading and sample drainage are recorded in real-time. If the consolidated drainage within 1 h is less than 0.1 cm^3, the sample consolidation is

considered to be completed. Then, under undrained conditions, the sample is loaded step by step according to the target dynamic stress amplitude. The dynamic load is applied step by step until the sample fails. The failure criterion is that the axial strain of the sample reaches $\varepsilon = 5\%$ under increasing cyclic load. The vibration wave adopts a sine wave, with 5 cycles of dynamic stress vibration at each level, and the loading frequency is 1 Hz.

The dry calcareous sand shall be screened before and after the test. The grading evolution curve shall be drawn, the relative crushing rate Br under each group of effective confining pressure shall be calculated and recorded, and the crushing rate shall be taken into account in the dynamic parameters of calcareous sand.

3. Test Results and Analysis

3.1. Effect of Effective Confining Pressure on Relationship between Dynamic Shear Modulus and Dynamic Shear Strain. By converting the dynamic elastic modulus obtained from the test, the dynamic shear modulus corresponding to different shear strains under effective confining pressure is obtained. It can be seen from Figure 4 that under the same confining pressure, the shear modulus G decreases with the increase of shear strain γ, and under the same shear strain, the dynamic shear modulus G increases with confining pressure. It is believed that as the effective confining pressure increases, the mutual extrusion between calcareous sand particles would be more serious. As a result, the skeleton is denser, and more contacts are generated, which, in turn, leads to larger stress of the sample and dynamic shear modulus. It can also be found from Figure 4 that if dynamic shear strain $\gamma < 0.4\%$, the decreasing rate of dynamic shear modulus with dynamic shear strain is faster and becomes slower with increasing dynamic shear strain.

3.2. Effect of Effective Confining Pressure on Relationship between Damping Ratio and Dynamic Shear Strain. According to the dynamic triaxial hysteretic cycle test results, the damping ratio curve of calcareous sand is obtained by the direct sorting method. As shown in Figure 5, it can be found that the damping ratio under the four groups of effective confining pressure increases with the increase of dynamic shear strain and gradually stabilizes, and the corresponding damping under high confining pressure is smaller than that under low confining pressure. Figure 6 shows the test sample under different cyclic loads with an effective confining pressure of 300 kPa. It can be found that with the increase of cyclic load, calcareous sand particles have an obvious sliding arrangement, and the contact friction between particles becomes closer. This violent physical effect causes greater deformation of the sample, resulting in greater energy consumption. Partial load-deformation curves of calcareous sand under each group of effective confining pressure are shown in Figure 7.

3.3. Effect of Effective Confining Pressure on Maximum Dynamic Shear Modulus of Calcareous Sand. The maximum dynamic shear modulus G_{max} of calcareous sand is a basic dynamic parameter of site effect analysis, which is the tangent slope of the backbone curve at the origin. It is related to the type of sand, average effective principal stress, dynamic shear strain amplitude, consolidation time effect, void ratio, and other factors. In this paper, the initial shear modulus G_0 corresponding to the minimum dynamic shear strain is taken as the maximum dynamic shear modulus.

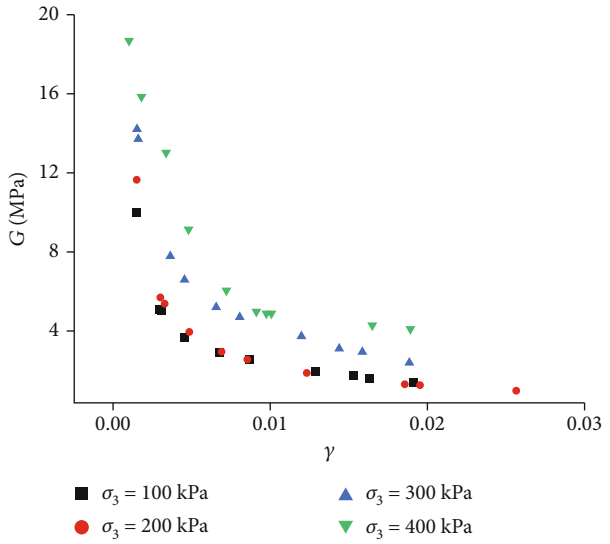

Figure 4: Relationship between shear modulus and shear strain.

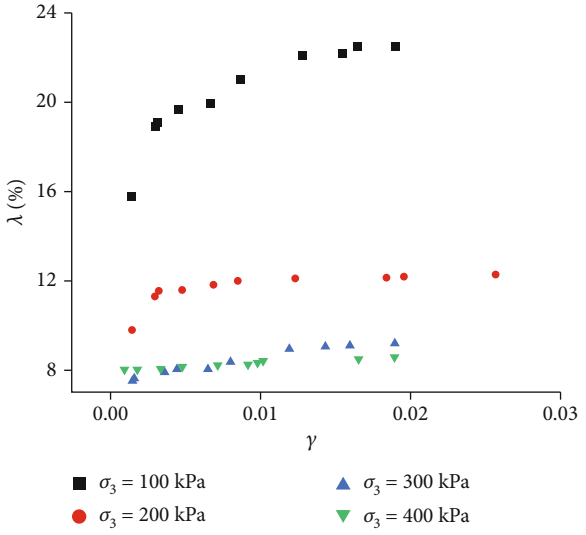

Figure 5: Relationship between damping ratio and shear strain.

According to the test results, the relationship curve between G_{max} and σ_m/p_a of calcareous sand is plotted in Figure 8.

It can be seen from Figure 8 that G_{max} of calcareous sand increases with increasing confining pressure, and can be described by Janbu [33] empirical formula (1).

$$G_{max} = Kp_a\left(\frac{\sigma_m}{p_a}\right)^n, \tag{1}$$

Figure 6: Sample diagram under different cyclic loads and 300 kPa effective confining pressure.

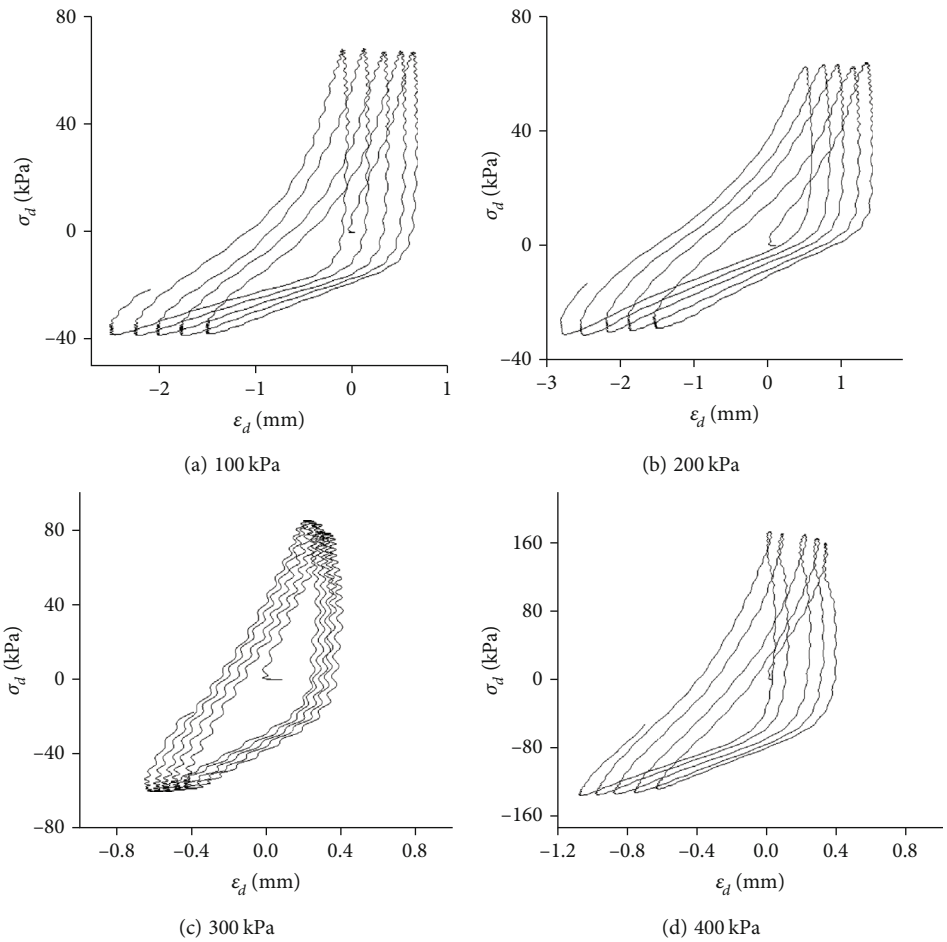

Figure 7: Load-deformation curves of calcareous sand under different effective confining pressures.

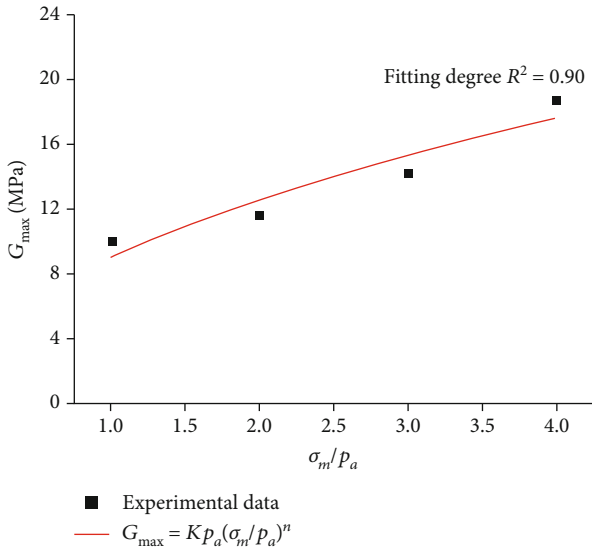

Figure 8: Calcareous calcareous sand $G_{max} \sim \sigma_m/p_a$ diagram.

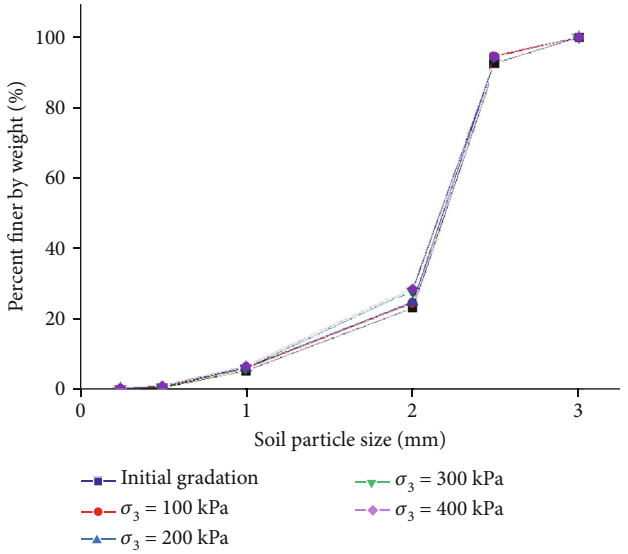

Figure 9: Grading curve of calcareous sand under different effective confining pressures.

where σ_m is the average effective consolidation stress. For the dynamic triaxial test, $\sigma_m = (\sigma_1 + 2\sigma_3)/3$, the stress state of the sample during consolidation is $\sigma_1 = \sigma_2 = \sigma_3$; that is, $\sigma_m = \sigma_3$, so we have:

$$G_{max} = Kp_a\left(\frac{\sigma_3}{p_a}\right)^n, \quad (2)$$

where K and n are two test parameters of soil, which can be determined by K the intercept and slope of the straight line on the longitudinal axis, respectively. The calcareous sand in this paper satisfies $K = 0.09017$ and $n = 0.48459$.

3.4. Particle Crushing of Calcareous Sand

3.4.1. Influencing Factors and Measurement of Particle Breakage. The crushing of calcareous sand particles is related to internal factors such as its location in the sea area, biogenesis, and its irregular shape. Meantime, it is also related to external factors such as particle gradation, relative compactness, porosity, and the type, time, stress state, and path of cyclic load applied during the test.

In this paper, the relative crushing rate *Br* proposed by Hardin [34] is used to measure the crushing of calcareous sand particles. Hardin defines the initial crushing potential B_{p0}, final crushing potential B_{pf}, and crushing amount B_t. Hardin believes that fine particles with particle size less than 0.074 mm have little effect on particle crushing. The crushing amount is the area difference between the front and back.

$$B_t = B_{p0} - B_{pf}. \quad (3)$$

The relative crushing rate *Br* is

$$B_r = \frac{B_t}{B_{p0}}. \quad (4)$$

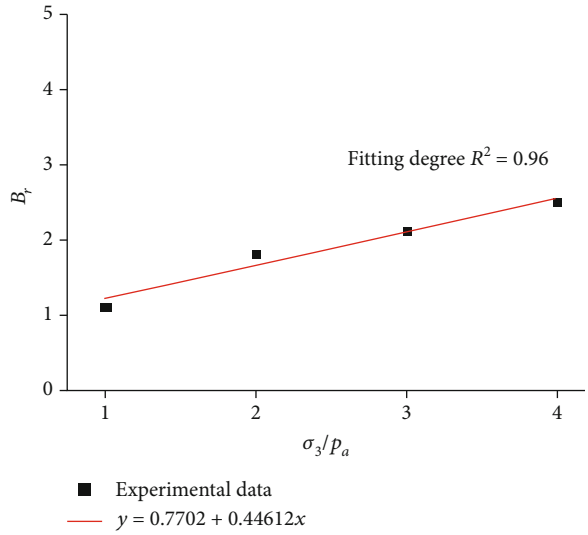

Figure 10: Calcareous sand $B_r \sim \sigma_3/p_a$ diagram.

3.4.2. Effect of Effective Confining Pressure on Particle Breakage of Calcareous Sand. Figure 9 shows the grading curve of samples before and after the test under different effective confining pressures. It can be found that with the increase of effective confining pressure, the particles of each particle group are broken to various degrees. The atmospheric pressure is 100 kPa.

It can be found in Figure 10 that the crushing rate *Br* and the effective confining pressure σ_3 show a good linear increasing relationship. The mathematical expression embracing the crushing rate *Br* and the effective confining pressure σ_3 can be obtained from the fitting curve Figure 11.

$$\frac{\sigma_3/p_a}{B_r} = a + b\frac{\sigma_3}{p_a}, \quad (5)$$

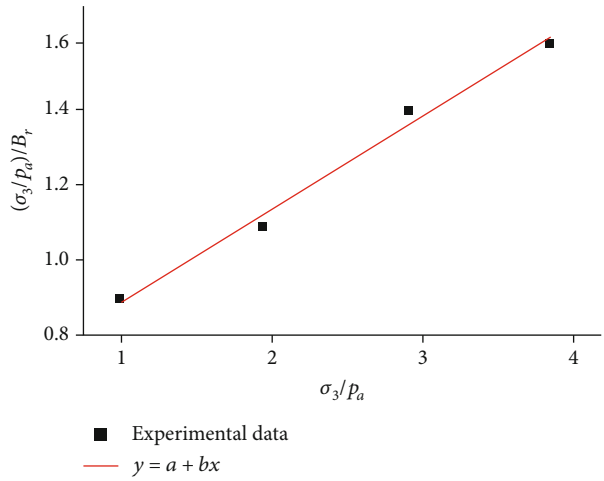

Figure 11: Calcareous sand $(\sigma_3/p_a)/B_r \sim \sigma_3/p_a$ diagram.

where a and b are the test parameters. For the calcareous sand studied in this paper, $a = 0.65$, and $b = 0.242$.

4. Dynamic Constitutive Correction of Equivalent Linear Model

4.1. Equivalent Linear Mode. Among many dynamic constitutive models, the Hardin-Drnevich equivalent viscoelastic linear model is widely used because of less dynamic parameters and clear physical meaning. The Hardin-Drnevich model adopts equivalent elastic modulus E or G and equivalent damping ratio λ to reflect the hysteresis and nonlinearity of the stress-strain relationship of sand and is expressed by the functional relationship between dynamic shear modulus and dynamic shear stress amplitude $G = G(\gamma_d)$ and the functional relationship between damping ratio and dynamic shear stress amplitude $\lambda = \lambda(\gamma_d)$, and the average effective consolidation stress is considered in the above functional relationship.

The equivalent modulus is obtained from the average slope of the hysteretic curve drawn under the vibration waveform of the weekly dynamic load.

$$E = \frac{\sigma_d}{\xi_d}, \tag{6}$$

$$G = \frac{\tau_d}{\gamma_d}. \tag{7}$$

σ_d and ξ_d represent the amplitude of dynamic stress and dynamic strain, respectively, and τ_d and γ_d represent the amplitude of dynamic shear stress and dynamic shear strain, respectively. The relationship between dynamic elastic modulus, dynamic shear modulus, and stress strain is converted by formulas (8) ~ (10). In this paper, the dynamic triaxial test, for the saturated sample, there is no volumetric strain during undrained loading, and the Poisson's ratio $\nu = 0.5$ can be assumed.

$$\tau_d = 0.5\sigma_d, \tag{8}$$

$$\gamma_d = \xi(1 + \nu), \tag{9}$$

$$G = \frac{\tau_d}{\gamma_d} = \frac{E}{2(1 + \nu)}. \tag{10}$$

In the Hardin-Drnevich equivalent viscoelastic linear model, the equivalent elastic modulus and stress-strain of sand under dynamic load can be expressed by hyperbola.

$$\tau_d = \frac{\gamma_d}{(1/G_0) + (\gamma_d/\tau_{d\,\max})}, \tag{11}$$

$$\frac{G}{G_0} = \frac{1}{1 + (\gamma_d/\gamma_r)}. \tag{12}$$

G_0 is the initial shear modulus (also the maximum shear modulus), $\tau_{d\,\max}$ is the maximum dynamic shear stress, and γ_r is the reference shear strain, which can be expressed as follows:

$$\gamma_r = \frac{\tau_{d\,\max}}{G_0}. \tag{13}$$

In the equivalent viscoelastic linear model, it can be considered that the damping ratio is the phenomenon of the energy consumption of geotechnical materials under dynamic load. It appears in the form of thermal energy, and the result is the attenuation of vibration. This energy consumption can be reflected by an equivalent damping ratio, as shown in formula (14), where ΔW is the energy consumed in one cycle and W is the total energy acting in one cycle.

$$\lambda = \frac{c}{c_{\mathrm{cr}}} = \frac{c}{2m\omega} = \frac{\psi}{4\pi} = \frac{1}{4\pi}\frac{\Delta W}{W}. \tag{14}$$

c is the damping coefficient, c_{cr} is the critical damping coefficient, and ψ is the number of energy losses.

$$\Delta W = \pi c\omega\varepsilon_{d0}^2 = S_{\mathrm{Hysteresis\,loop}}, \quad W = 0.5\sigma_{d0}\varepsilon_{d0} = A_0. \tag{15}$$

Here, A_0 is the triangle area under the connecting line from the origin to the maximum amplitude point $(\sigma_{d0}, \varepsilon_{d0})$, so there is:

$$\lambda = \frac{1}{4\pi}\frac{\Delta W}{W} = \frac{1}{4\pi}\frac{S_{\mathrm{Hysteresis\,loop}}}{A_0}. \tag{16}$$

4.2. Modification of Equivalent Linear Model. The Hardin-Drnevich equivalent viscoelastic linear model considers the average effective consolidation stress in the functional relationship of dynamic shear modulus. Through a large number of dynamic triaxial tests and screening experiments, the functional formula between particle breakage rate Br and average effective consolidation stress is established, and the particle breakage rate Br is taken as an intermediate quantity of dynamic constitutive correction. The maximum dynamic shear modulus $G_{\max}$ (also known as the initial shear modulus G_0) in the equivalent viscoelastic linear model is modified by the particle crushing formula; that is, the particle crushing formula (5) and the maximum dynamic shear modulus formula (2) are combined and substituted into the equivalent viscoelastic linear model to

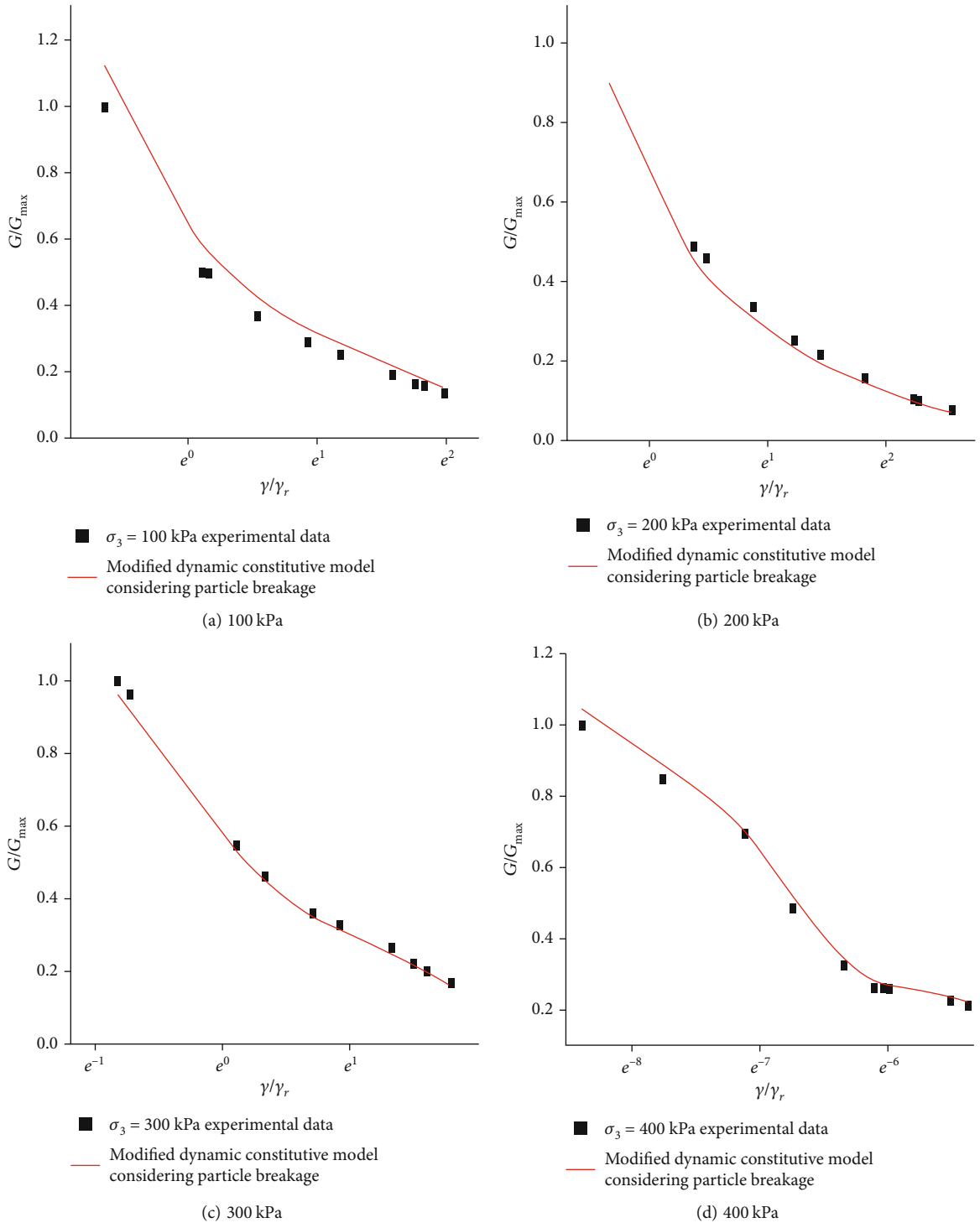

Figure 12: Comparison diagram of $G/G_{max} \sim \gamma/\gamma_r$ fitting for calcareous sand under different effective confining pressures.

obtain an equivalent linear dynamic constitutive model considering particle crushing (17).

$$\frac{G}{G_0} = \frac{G}{Kp_a(\sigma_m/\rho_a)^n} = \frac{G}{Kp_a(\sigma_3/\rho_a)^n} = \frac{G}{Kp_a(aB_r/(1-bBr))^n} = \frac{1}{1+(\gamma/\gamma_r)}. \tag{17}$$

The above dynamic constitutive model contains four parameters, which are divided into the following two groups: ① Parameters K and n are related to dynamic shear modulus. ② Parameters a and b are related to effective principal stress and particle crushing rate Br. The specific determination methods of these parameters are as follows:

(1) Parameters K and n are related to dynamic shear modulus. The $G_{max} \sim \sigma_m/p_a$ test point of the

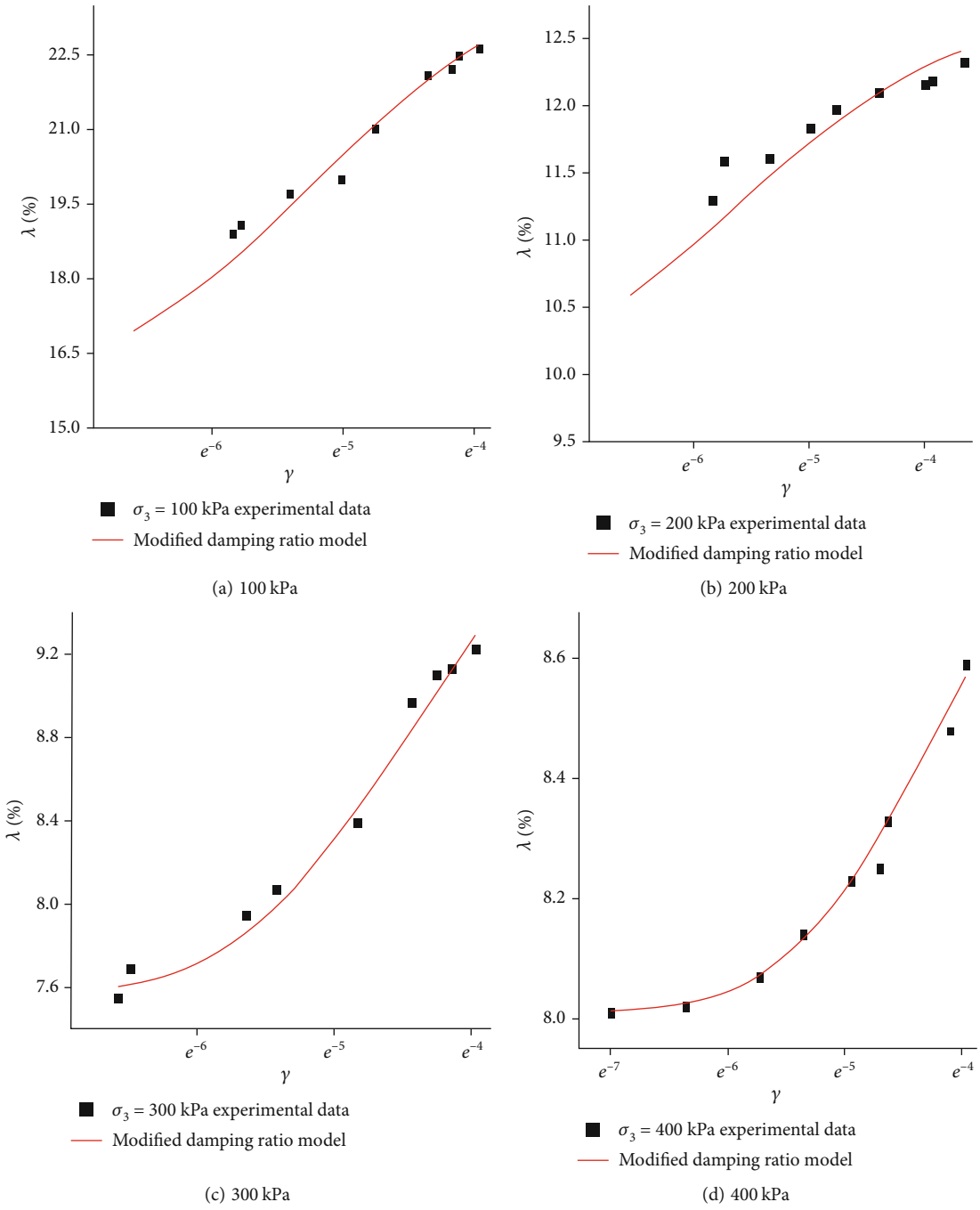

Figure 13: Comparison diagram of $\lambda \sim \gamma$ fitting for calcareous sand under different effective confining pressures.

dynamic triaxial test of calcareous sand is drawn in the plane coordinate system, and the intercept and slope of the fitting line on the longitudinal axis are K and n

(2) Particle crushing rate Br. The calcareous sand samples before and after the dynamic test are dried and cooled to normal temperature, the screening test is conducted to obtain the particle size curve before and after the test, and the integral area of particle size curve under each group of effective confining pressure is calculated. The particle crushing rate Br is obtained by substituting the crushing potential and crushing amount formula defined by Hardin

(3) Parameters a and b are related to effective principal stress and particle breakage Br. The $(\sigma_3/p_a)/B_r \sim \sigma_3/p_a$ test point of dynamic triaxial test of calcareous sand is drawn in the plane coordinate system, and the intercept and slope of the fitting line on the longitudinal axis are a and b

4.3. Verification of Equivalent Linear Model. The modified equivalent viscoelastic linear model considering particle breakage is used for calculation and compared with the test results. Figure 12 shows the comparison diagram of $G/G_{max} \sim \gamma/\gamma_r$ fitting under effective confining pressures of 100 kPa, 200 kPa, 300 kPa, and 400 kPa.

It can be found from Figure 12 that under each effective confining pressure, the modified equivalent linear model is consistent with the test point, with a good correlation. With the gradual increase of dynamic shear strain γ, the dynamic shear modulus ratio G/G_{max} gradually decreases, and the attenuation rate gradually increases.

4.4. Damping Ratio Fitting in Equivalent Linear Model. The experimental research shows that the variation law of damping ratio of calcareous sand with shear strain is relatively complex, and the direct description error of damping ratio formula (18) of Hardin-Drnevich equivalent viscoelastic linear model is large. Here, the damping ratio formula (19) modified by Chen and Zhuang [35] is used for fitting.

$$\frac{\lambda}{\lambda_{max}} = 1 - \frac{1}{1 + (\gamma/\gamma_r)}, \tag{18}$$

$$\lambda = \lambda_{min} + \lambda_0 \left(1 - \frac{G}{G_{max}}\right)^n. \tag{19}$$

Combined with the dynamic shear modulus ratio formula (12) of the H-D equivalent viscoelastic linear model, the damping ratio model formula (20) is modified by the H-D equivalent viscoelastic linear model.

$$\lambda = \lambda_{min} + \lambda_0 \left(\frac{\gamma}{\gamma + \gamma_r}\right)^n. \tag{20}$$

In formula (20), λ_{min} is the minimum damping ratio, and λ_0 and n are fitting parameters related to sand properties. The modified damping ratio formula of the H-D equivalent viscoelastic linear model is used for calculation and compared with the test results. The following shows the comparison diagram of $\lambda \sim \gamma$ fitting under four groups of effective confining pressures of 100 kPa, 200 kPa, 300 kPa, and 400 kPa, as shown in Figure 13.

It can be found from the figure that the H-D equivalent viscoelastic linear model is used to modify the damping ratio model to fit the test data, and the data points under different effective confining pressures basically fall near the fitting curve. Therefore, formula (20) is effective to describe the relationship between damping ratio and shear strain.

5. Conclusion

Taking the calcareous sand at the South China Sea Islands and reefs as the research material, this paper carries out consolidated undrained dynamic triaxial test to study the dynamic parameters such as dynamic shear modulus and damping ratio of calcareous sand and particle breakage in the test. A modified dynamic constitutive model of calcareous sand is studied considering particle breakage, and the following conclusions are obtained:

(1) The initial shear modulus increases with increasing effective confining pressure; the effective confining pressure is constant, the dynamic shear modulus decreases with the increase of dynamic shear strain, and the attenuation rate gradually stabilizes. With the increase of dynamic shear strain, the damping ratio increases as a whole

(2) The test shows that the particle content of the coarse-grained group is decreasing and that of the fine-grained group is increasing during the continuous application of cyclic dynamic load. As the effective confining pressure increases step by step, the particle breakage becomes more significant, and when the effective confining pressure increases to a certain extent, the increase of the crushing amount of calcareous sand decreases and gradually stabilizes

(3) By establishing the particle crushing function formula of particle crushing and average effective consolidation stress of calcareous sand and taking it as the intermediate quantity, the maximum dynamic shear modulus in the Hardin-Drnevich equivalent viscoelastic linear model is modified, and then, a modified dynamic constitutive model considering particle crushing is obtained. By comparing with the experimental data, it is found that the calculated value of the modified dynamic constitutive model is in good agreement with the experimental value, and the relative error is no more than 12%, and the average error is no more than 8%, which can better predict the dynamic characteristics of calcareous sand. The modified dynamic constitutive model is suitable for the dynamic response of calcareous sand considering particle breakage under graded loading in the dynamic load test

Data Availability

The data are generated from experiments and can be available from the corresponding author upon request.

Conflicts of Interest

The authors declare that there are no conflicts of interest regarding the publication of this paper.

Acknowledgments

This work was supported by A Study on the Instability Mechanism of Steel Cylinder Retaining Structure in Calcareous Sand under Transverse Dynamic Load.

References

[1] R. Wang and W. Wenjuan, "Exploration and research on geotechnical engineering geology of coral reef –30 years of coral

reef research," *Journal of Engineering Geology*, vol. 27, no. 1, pp. 202–207, 2019.

[2] H. Zhao and L. Wang, "Study on the construction of artificial coral reefs in the South China Sea," *Tropical Geography*, vol. 37, no. 5, pp. 681–693, 2017.

[3] Y. Kefu, G. Zhang, and R. Wang, "Coral reefs in the South China Sea: from global change to oil and gas exploration – a special review of the third Earth System Science Conference," *Progress in Geoscience*, vol. 29, no. 11, pp. 1287–1293, 2014.

[4] X. Wang, "Engineering geological characteristics of Spratly Islands coral reef and feasibility study of large-scale engineering construction," *Graduate School of Chinese Academy of Sciences (Wuhan Institute of Geotechnical Mechanics)*, 2008.

[5] Z. Yuan, Y. Kefu, and Y. Wang, "Research progress on engineering geological characteristics of coral reef rock and soil," *Tropical Geography*, vol. 36, no. 1, pp. 87–93, 2016.

[6] W. Yang, C. Jie, and L. Neng, "Experimental study on the mechanical behavior and particle breakage characteristics of hydraulic filled coral sand on a coral reef island in the South China Sea," *Rock and Soil Mechanics*, vol. 41, no. 10, pp. 3181–3191, 2020.

[7] J. Ma, X. L. Li, J. G. Wang et al., "Experimental study on vibration reduction technology of hole-by-hole presplitting blasting," *Geofluids*, vol. 2021, 2021.

[8] J. Wang, T. Zuo, X. Li, Z. Tao, and J. Ma, "Study on the fractal characteristics of the pomegranate biotite schist under impact loading," *Geofluids*, vol. 2021, 2021.

[9] W. Hao, G. Zhao, and S. Ma, "Failure behavior of horseshoe-shaped tunnel in hard rock under high stress: phenomenon and mechanisms," *Transactions of Nonferrous Metals Society of China*, vol. 32, no. 2, pp. 639–656, 2022.

[10] G. R. Martin, W. D. L. Finn, and H. B. Seed, "Effects of system compliance on liquefaction tests," *Journal of Geotechnical Engineering Division*, vol. 104, no. 4, pp. 463–479, 1978.

[11] W. Li and W. Wang, "Nonlinear dynamic shear strain model of cohesionless soil," *Journal of water conservancy.*, vol. 9, pp. 11–17, 1993.

[12] J. Zhao, W. Wang, Y. Chang, and N. Chen, "Three dimensional true nonlinear seismic response analysis method and model test verification of high concrete face dam," *Journal of water conservancy.*, vol. 9, pp. 12–18, 2003.

[13] B. O. Hardin and V. P. Drnevich, "Shear modulus and damping in soils: design equations and curves," *Journal of the Soil Mechanics and Foundation Division, ASCE*, vol. 98, no. 7, pp. 667–692, 1972.

[14] K. Ishihara, N. Yoshida, and S. Tsujino, "Modeling of stress-strain relations of soils in cyclic loading," *Proceedings of the Fifth International Conference on Numerical Methods in Geomechanics*, vol. 1, pp. 373–380, 1985.

[15] G. Chen, X. Liu, and D. Zhu, "Experimental study on dynamic shear of newly deposited soil in the south of the Yangtze River in Jiangsu Province," *Journal of underground space and engineering*, vol. 4, pp. 163–168, 2007.

[16] R. Liu, H. Hou, Y. Chen, P. Ming, and X. Zhu, "Elastoplastic constitutive model of coral sand considering particle breakage based on unified hardening parameter," *Marine Georesources and Geotechnology*, vol. 51, no. 1, pp. 1–24, 2021.

[17] T. J. Chen and T. S. Ueng, "Energy aspects of particle breakage in drained shear of sands," *Géotechnique*, vol. 50, no. 1, pp. 65–72, 2015.

[18] B. O. Hardin, "Crushing of soil particles," *Journal of Geotechnical Engineering*, vol. 111, no. 10, pp. 1177–1192, 1985.

[19] G. Wang, Z. Wang, Q. Ye, and X. Wei, "Particle breakage and deformation behavior of carbonate sand under drained and undrained triaxial compression," *International Journal of Geomechanics*, vol. 20, no. 3, p. 04020012, 2020.

[20] R. Wang and J. Sun, "Damage slip coupling analysis of undrained behavior of calcareous sand," *Journal of water conservancy*, vol. 7, pp. 75–78, 2002.

[21] Z. Cai, H. Hou, and J. Zhang, "Study on critical state and constitutive model of coral sand considering the influence of particle breakage," *Journal of Geotechnical Engineering*, vol. 41, no. 6, pp. 989–995, 2019.

[22] B. Hu, "Study on crushing mechanical properties and constitutive model of calcareous sand particles under triaxial conditions," *Graduate School of Chinese Academy of Sciences (Wuhan Institute of Geotechnical Mechanics)*, pp. 1–107, 2008.

[23] Y. Wang, Z. G. YiHong, and L. Wang, "Mechanical properties of macro meso crushing of calcareous sand in the South China Sea," *geotechnical mechanics*, vol. 39, no. 1, pp. 200–206, 2018.

[24] P. Yu, X. Ding, Y. Xiao, J. Chu, and W. Deng, "Study on particle breakage characteristics of calcareous sand based on dyeing calibration and image particle segmentation," *geotechnical mechanics*, vol. 40, no. 7, pp. 2664–2672, 2019.

[25] H. B. Seed, R. T. Wong, I. M. Idriss, and K. Tokimatsu, "Moduli and damping factors for dynamic analyses of cohesionless soils," *Journal of Geotechnical Engineering, ASCE*, vol. 112, no. 11, pp. 1016–1032, 1986.

[26] B. O. Hardin and W. L. Black, "Vibration modulus of normally consolidated clay," *Journal of the Soil Mechanics and Foudations Engineering Division, ASCE*, vol. 94, no. 2, pp. 353–369, 1968.

[27] L. Zhu and W. Xiaofeng, "Study on dynamic characteristics of sand under low amplitude shear strain," *Dam observation and geotechnical test*, vol. 12, no. 1, pp. 27–33, 1988.

[28] Z. Shen, "Indoor measurement of dynamic deformation calculation parameters of sand," *Scientific research on water conservancy and transportation*, vol. 2, pp. 10–17, 1984.

[29] W. Dong, S. Sun, and Y. Yuzhen, "Large scale triaxial experimental study on dynamic deformation characteristics of rockfill," *Geotechnical mechanics*, vol. 32, no. add 2, pp. 2731–2734, 2011.

[30] Y. Jafarian, H. Javdanian, and A. Hadda, "Dynamic properties of calcareous and siliceous sands under isotropic and anisotropic stress conditions," *Soils and Foundations*, vol. 58, no. 1, pp. 172–184, 2018.

[31] R. Gao and J. Ye, "Experimental study on dynamic characteristics of calcareous sand blowing island reef in the South China Sea," *Rock and Soil Mechanics*, vol. 40, no. 10, pp. 3897–3908, 2019.

[32] M. Gao, X. Peng, and Q. Chen, "Triaxial experimental study on dynamic characteristics of unsaturated calcareous sand in the South China Sea," *Journal of Beijing University of Technology*, vol. 47, no. 6, pp. 625–634, 2021.

[33] M. Luan, Y. He, and X. Chengshun, "Experimental study on cyclic shear characteristics of silt in the Yellow River Delta," *Geotechnical mechanics*, vol. 29, no. 12, pp. 3211–3216, 2008.

[34] B. O. Hardin, "The nature of stress-strain behaviour for soils," in *Proceedings of Specialty Conference on Earthquake Engineering and Soil Dynamics*, pp. 3–90, ASCE, New York, 1978.

[35] G. Chen and H. Zhuang, "Study on dynamic constitutive relationship and parameters of soil based on Davidenkov skeleton curve," *Journal of Geotechnical Engineering*, vol. 27, no. 8, pp. 860–864, 2005.